

# Isothermal viscoelastic properties of PMMA and LDPE over 11 decades of frequency and time: a test of time–temperature superposition

Julie Capodagli · Roderic Lakes

Received: 24 September 2007 / Accepted: 15 April 2008 / Published online: 13 June 2008  
© Springer-Verlag 2008

**Abstract** Many instruments used to measure viscoelastic properties are only capable of subjecting a sample to a limited range of loading frequencies. For thermorheologically simple materials, it is assumed that a change in temperature is equivalent to a shift of the viscoelastic behavior on the log frequency or time axis. For many materials, time–temperature superposition appears to work well for modulus or compliance curves over three decades of time or frequency, but some deviations are known if the window is expanded to five or six decades. To apply a more stringent test of the validity of time–temperature superposition, broadband viscoelastic spectroscopy is used to isothermally study polymethylmethacrylate and low-density polyethylene at several temperatures in the glassy region. Shear modulus and damping ( $\tan \delta$ ) are measured isothermally over a wide range (up to 11 decades) of time and frequency. Results indicate that, while modulus curves can be approximately superimposed, the damping ( $\tan \delta$ ) curves change in height and shape with temperature.

**Keywords** Time-temperature superposition · Complex modulus · Constitutive equation · Viscoelasticity

## Introduction

Polymers are highly viscoelastic materials, so the mechanical properties vary widely depending on the duration or frequency of the applied stress. This time-dependent behavior is significant in typical engineering applications. For this reason, it is desirable to devise a method that can predict the viscoelastic behavior of polymeric materials over time scales that extend as long as the working life of the material or to predict behavior at frequency too high to easily handle in the laboratory. Since it is normally difficult to either perform such a lengthy creep or relaxation test or to test a specimen over a wide range of loading frequencies, inferential methods are used to determine the time-dependent behavior of viscoelastic materials. In particular, time–temperature superposition is used to obtain an extended range of time or frequency.

The notion of time temperature shift is expressed as follows, with  $G(t, T)$  as shear modulus which depends on time  $t$  and temperature  $T$ .

$$G(t, T) = G(\zeta, T_0), \text{ with } \zeta = \frac{t}{a_T(T)} \quad (1)$$

in which  $\zeta$  is the reduced time,  $T_0$  is the reference temperature, and  $a_T(T)$  is the shift factor. In addition to these horizontal shifts on the log time axis, vertical shifts on the modulus axis are also incorporated as described below. Two models are normally used for the shifting along the log frequency or time axis. The first is the Arrhenius form given in Eq. 2, based on the Zener model which describes the relaxation of a viscoelastic material as the sum of independent relaxation

J. Capodagli · R. Lakes (✉)  
Department of Engineering Physics,  
University of Wisconsin-Madison,  
541 Engineering Research Building,  
1500 Engineering Drive, Madison,  
WI 53706-1687, USA  
e-mail: lakes@engr.wisc.edu

processes that are a result of various sources of internal friction (McCrum et al. 1997):

$$a_T(T) = \exp \left\{ \left[ \frac{\Delta H}{R} \right] \left[ \frac{1}{T} - \frac{1}{T_0} \right] \right\} \quad (2)$$

in which  $\Delta H$  is the activation energy associated with a mechanism of internal friction,  $R$  is the gas constant, and  $T_0$  is the reference temperature chosen for the master curve. In polymers, the Arrhenius form may be applicable to relaxations below the glass transition temperature in amorphous polymers and to some relaxations in crystalline polymers (McCrum et al. 1997). The WLF equation of Williams, Landel, and Ferry (Ferry 1970) models the shift factor for many polymers:

$$\log a_T(T) = -\frac{C_1(T - T_0)}{C_2 + (T - T_0)} \quad (3)$$

The WLF equation describes the effect of temperature on the shift factor quite well for many polymers near the glass–rubber transition.  $C_1$  and  $C_2$  are empirically determined constants that depend on the type of polymer. The WLF form coincides with the Arrhenius form for  $C_2 = T_0$  and  $C_1 = (\Delta H/R)/(T_0 \ln 10)$ .

The basic horizontal shifts have been supplemented for polymers with vertical shifts of the modulus. For example, according to the Rouse model (Ferry 1970), the modulus is multiplied by a factor  $b_T$ :

$$b_T = \frac{T_0 \rho_0}{T \rho} \quad (4)$$

The temperature ratio represents an effect of entropy-based restoring force in the flexible chains and the ratio of density  $\rho$  represents an effect of thermal expansion. This modulus shift factor is, in some but not all cases, only weakly dependent on temperature and is often neglected (Wood-Adams and Costeux 2001). There are many materials with different vertical shifts.

For thermorheologically simple materials (those which obey time–temperature superposition), a change in temperature is equivalent to a shift in the material's behavior on the log time or frequency axis. Such a shift can be interpreted as evidence that the temperature changes are effectively accelerating or retarding the dominant viscoelastic process or processes, because a shift on a log scale is equivalent to multiplying the scale by a number. Viscoelastic property tests are performed on a specimen over a range of temperatures and the results are used to extrapolate the behavior of the material at room temperature for short or long time periods that are difficult or impossible to attain experimentally. This is done by measuring the viscoelastic properties of the material over a range of two or three decades of frequency or time and plotting the curves.

Material properties over a wide range are determined by superimposing these curves by shifting them along the log frequency or log time axis to construct a master curve that spans a much greater window of frequency or time.

The first published master curves were compiled from viscoelastic measurements of polyisobutylene by Tobolsky and Andrews (1945). Ferry (1950) presented the theory for the temperature superposition process. This work stimulated many experimental studies of this aspect of polyisobutylene, all of which appeared to support the concept of time–temperature superposition. The combined data from these studies spanned a range of 15 decades in reduced time/frequency (Marvin 1953). The agreement of the various data sets was taken as evidence that all of the molecular mechanisms involved in the deformation process had the same temperature dependence.

Since these publications, many types of polymers have been assumed to be thermorheologically simple. Time–temperature superposition has been widely used to extrapolate their mechanical properties. However, departures from superposition were observed in several materials by Plazek (1980) and Cavaille et al. (1987). Plazek observed that if data are available over a relatively narrow experimental window, three decades or less, the test for thermorheological simplicity can only be definitive in its failure. Such an experiment is capable of demonstrating thermorheological complexity but it cannot demonstrate simplicity. Plazek showed that nearly perfect superposition was obtained for data for polystyrene over a restricted range of 3.4 decades, but that curves over six decades could not be superposed. Thermorheological complexity was even discovered in polyisobutylene, the most standard example of successful time–temperature superposition. Measurements of polyisobutylene's compliance over five decades of time indicate that the compliance can be extrapolated accurately using time–temperature superposition. However, measurements of the loss tangent at various temperatures over seven decades of frequency show that the shape of the damping peak changes with temperature (Plazek et al. 1995). Further, particulars for the polymers studied here are presented in the “[Results and discussion](#)” section.

Despite these caveats, time–temperature superposition has been widely used to extrapolate the viscoelastic properties of polymers over a range of time or frequency beyond what can be measured by commercially available testing devices. Extrapolation to 12 or more decades is commonly done. However, a critical test of this method has been limited either by the duration of the experiment or the range of loading frequencies

the apparatus can provide. Most of the commercially available test devices are only capable of measuring a few decades of frequencies. Such experiments can only demonstrate that a polymer is thermorheologically complex by measuring deviations from the predicted behavior of the material based on time–temperature superposition. They cannot prove that a material is thermorheologically simple. Specifically, a material may appear thermorheologically simple if the frequency range is insufficient or data evaluation is insufficient. It may also appear thermorheologically complex as a result of experimental error. Time–temperature superposition can fail if the material undergoes a phase transformation in the temperature range of interest. Thermorheological complexity can also arise in heterogeneous solids in which two or more relaxation processes are simultaneously present which follow different temperature dependencies. For example, a material for which a dominant relaxation mechanism is not thermally activated, as in thermoelastic damping or in damping due to stress-induced fluid flow in porous solids, is expected to be thermorheologically complex. Indeed, in the study of secondary transitions, Heijboer (1977) recognized the importance of measurements over a wide frequency range and suggested the use of multiple instruments to achieve such a range.

In the present work, broadband viscoelastic spectroscopy (BVS) is used to make a stringent test of time–temperature superposition. The BVS apparatus is capable of measuring viscoelastic properties over as much as 11 decades of time and frequency, isothermally, without appeal to time–temperature superposition. The present work compares viscoelastic measurements over a wide range of frequencies at various temperatures to evaluate the applicability of time–temperature superposition for an amorphous polymer, polymethylmethacrylate (PMMA) and a crystalline polymer, low-density polyethylene (LDPE).

## Experimental

### Materials

Commercial polymethyl methacrylate rods and low-density polyethylene rods were obtained from Cope Plastics Inc., Godfrey, IL, USA. The PMMA rods were initially 3.33 mm in diameter and 1.8 m in length, with a density of 1.15 g/cm<sup>3</sup>. The polyethylene rods were initially 6.72 mm in diameter and 3 m in length, with a density of 0.94 g/cm<sup>3</sup>. Test specimens were cut from these rods and ground to length. BVS specimen lengths varied depending on the type of test, the frequency

range investigated, and the temperature of the test; they were from 10 to 30 mm. Specimens for resonant ultrasound spectroscopy were prepared with length equal to diameter (3.33 mm for PMMA), to facilitate interpretation.

### Methods

Measurements of complex dynamic shear modulus, shear creep compliance, and loss tangent were made using the BVS (Fig. 1) (Brodt et al. 1995; Lee et al. 2000). BVS involves examining the resonant, sub-resonant, and transient behavior of a specimen of material fixed at one end and free at the other and excited by torque at the free end in either torsion or bending. The wide range of time and frequency is obtained by eliminating resonances from the devices used for loading and for displacement measurement, by minimizing the inertia attached to the specimen, and by use of a geometry giving rise to a simple specimen resonance structure amenable to simple analysis. The limit at long time/low frequency (at room temperature) is based on the experimenter's patience. The limit at high frequency is based on the ratio of signal to noise in high harmonic resonances.

The BVS apparatus is isolated from building vibration noise by a damped spring mass system. The apparatus is contained within a massive brass chamber orders of magnitude more stiff than the specimens studied. Low-frequency noise due to room air currents

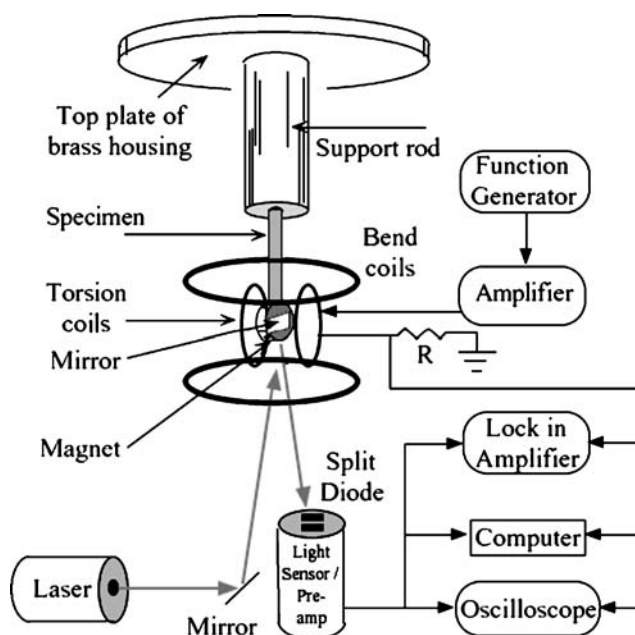


**Fig. 1** Schematic diagram of broadband viscoelasticity spectrometer (BVS) after Lakes (1999)

is excluded by enclosing the apparatus in a baffle. Static magnetic fields which might perturb creep measurements are excluded by a mu metal magnetic shield. Each specimen was cemented to a metal support rod, brass in this case, 12.7 mm in diameter, with structural stiffness orders of magnitude greater than that of the specimen. An alumina offset was used between specimen and rod to minimize heat conduction in experiments above or below ambient temperature.

The torque  $M^*$  is applied to the free end of the specimen by an electric current through a Helmholtz coil, generating a magnetic field. This field acts upon a high-intensity neodymium iron boron magnet attached to the specimen. The voltage signal which represents the torque is taken across a known non-inductive resistor in series with the Helmholtz coil. Calibration of the torque signal is performed using the well-characterized 6061-T6 aluminum alloy ( $G = 25.9$  GPa,  $\tan \delta \approx 3.6 \times 10^{-6}$ ). The electromagnetic natural frequency of the coil is several megahertz, well above the frequency range studied. The angular displacement  $\theta$  of the specimen is measured using light from a diode laser reflected from a mirror mounted on the magnet to a split-diode light detector. Time delay due to the speed of light gives rise to a bandwidth in the GHz region, far above the frequency range studied. The detector signal is amplified with a wide band (DC to several MHz) differential amplifier. This amplifier is built into a small circuit box immediately behind the detector. The rationale for this arrangement is to avoid cable capacitance which would introduce phase errors. The detector–preamplifier assembly is mounted on a small micrometer-driven stage used for in situ calibration of the detector system. Calibration is done by preparing a plot of output voltage vs. micrometer displacement. In dynamic (sinusoidal) experiments, the phase angle between torque and angle is determined using a lock-in amplifier (Stanford Research Systems SRS 850) with claimed phase resolution  $0.001^\circ$ . The frequency range for scans was segmented since the wide frequency range necessitates different time constant settings. For frequency sufficiently below the first natural frequency, torsional stiffness is given by  $|G^*| \approx K \frac{|M^*|L}{\theta}$ , and loss by  $\tan \delta \approx \tan \phi$  in which  $K$  is a geometrical factor for torsion  $L$  is specimen length, and  $\phi$  is the observed phase difference between the torque and angle signals. In the sub-resonant domain, the lumped relation  $\tan \delta = \tan \phi(1 - (\omega / \omega_0)^2)$  is used, with  $\omega_0$  as the fundamental resonance angular frequency. Below the fundamental resonance, it is a good approximation to the exact form for a distributed system.

The BVS apparatus is also capable of transient creep tests, limited by patience to several days. Creep

experiments are done by applying an electrical step function to the Helmholtz coil. Creep data are captured via a digital oscilloscope. Since the slopes of the creep curves were relatively small in the glassy region,  $\tan \delta$  (for corresponding low frequency) was calculated from creep by fitting a power law  $J(t) = At^n$  to segments of the creep curve and applying the corresponding approximate interrelation. Specifically,  $J'(\omega)|_{\omega=1/t} \approx J(t)$  so in the plots, direct dynamic results, and creep results are shown on complementary scales in which time is transformed into effective frequency via  $t = 1 / 2\pi\nu$ . Mechanical damping was determined from the slope  $n$  of power law creep fits by  $\delta \approx \frac{n\pi}{2}$ .

This fixed-free torsion pendulum configuration possesses a small inertia, and so the first natural resonance frequency of the specimen is high, 3–15 kHz depending on the specimen and temperature. Higher resonant modes are used, via the method of resonance half width, to determine viscoelastic properties at their respective frequencies. The upper frequency limit is about 100 kHz, depending on the type of specimen.

Resonant ultrasound spectroscopy (RUS) was used to determine the dynamic modulus and damping capacity at 200 kHz for PMMA; the LDPE did not provide a signal sufficient for interpretation. A specimen with length equal to diameter was held by its edges between two shear ultrasonic transducers. Frequency was varied through the fundamental natural frequency, at room temperature. Modulus was inferred via the exact analytical solution for torsional vibration of a cylinder free at both ends. The mode structure was used to identify the fundamental frequency. Damping was inferred via the method of resonant half width. At the resonance angular frequencies  $\omega_0$  in both BVS and RUS, damping was calculated using the width  $\Delta\omega$  at half maximum as follows:

$$\tan \delta \approx \frac{1}{\sqrt{3}} \frac{\Delta\omega}{\omega_0}. \quad (5)$$

Specimens of PMMA and LDPE in BVS experiments were cooled or heated to temperatures ranging from 6 to  $80^\circ\text{C}$  by passing an air stream through a temperature control module connected to the sample chamber. The module consists of two lines of copper tubing wound into three turns and soldered together with pipe solder. One of these lines is used to conduct the air flow to the sample. Chiller-cooled water–antifreeze mixture is pumped through the other line during experiments below room temperature. The air flow is directed from the copper pipe into a ceramic tube which contains a heating element constructed of NiCr wire wrapped around a piece of  $\text{Al}_2\text{O}_3$  (alumina ceramic) foam. For experiments above room temperature, electric current

is passed through the NiCr wire which heats the air flow. The high temperature limit was based on the stability of specimens free at one end when they soften as the glass transition is approached. A further limit is imposed by the temperature rating (95°C) of the cyanoacrylate adhesive used to cement the sample to the support rod. The frequency range in the elevated temperature studies was limited by noise generated by the turbulence in the hot air current used to heat the sample. Creep tests at elevated temperatures were conducted over a lesser period of 4 to 6 h, owing to limited stability of the fixed-free configuration when the specimen softens.

## Results and discussion

The room temperature results in Fig. 2 show the full  $\beta$  damping peak in PMMA. Differentiation of creep results to obtain a slope introduces noise, hence the scatter in the damping values obtained from creep. The damping peak occurs near 1 Hz at room temperature in agreement with prior studies. The extensive frequency range of these results allows one to recognize that the  $\beta$  peak is much wider than a Debye peak (also shown in the figure) corresponding to a single relaxation time. This  $\beta$  peak has been previously measured in PMMA by Koppelman (1958) using several

different isothermal loading devices in order obtain measurements spanning seven decades in frequency. The LDPE room temperature curves show a portion of the large  $\alpha$  peak that dominates the low-frequency region of the spectrum as well as a portion of the  $\beta$  peak which becomes apparent in the high-frequency portion of the spectrum. Similar peaks have been observed (Flocke 1962) in dynamic temperature sweeps, where the sample is oscillated at a single frequency and the sample temperature is varied.

To compare these results to results of previous experiments in time–temperature superposition, the full data sets are truncated to mimic the limited frequency window available to traditional dynamic testing devices. Specifically, the abbreviated frequency range is 0.01–10 Hz, representative of the frequency range typically implemented in commercial dynamic testing apparatuses. The results are plotted on a log–log graph and shifted horizontally until the best alignment of the shear modulus curves is achieved to form a master curve, as shown in Fig. 3. A reference temperature  $T_0 = 23^\circ\text{C}$  was chosen so that the resulting master curve can be compared to the isothermal broadband results at room temperature. It was possible to align the modulus curves to create a reasonable master curve. The loss tangent curves, by contrast, do not shift by the same amount; moreover, the peak height varies with temperature. This becomes more evident when the full

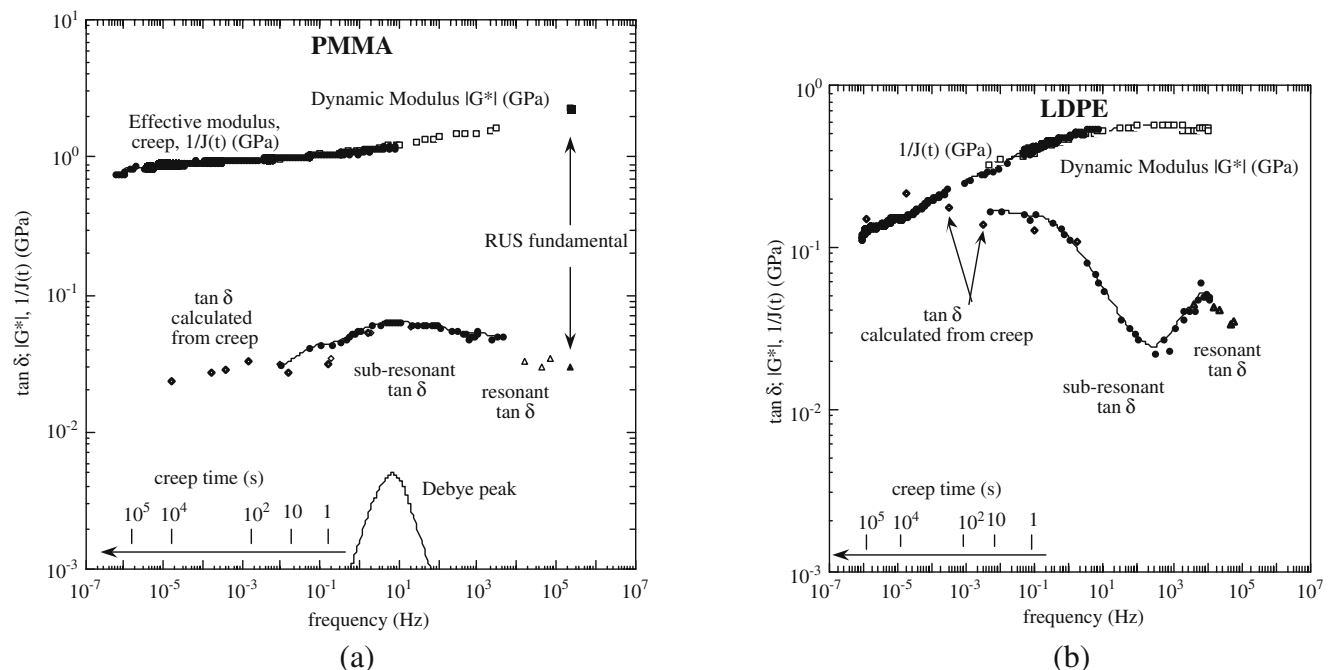


**Fig. 2** Room temperature isothermal modulus and damping measurements of PMMA (a) and LDPE (b). No time temperature shifts were used. *Triangles*: damping via resonance

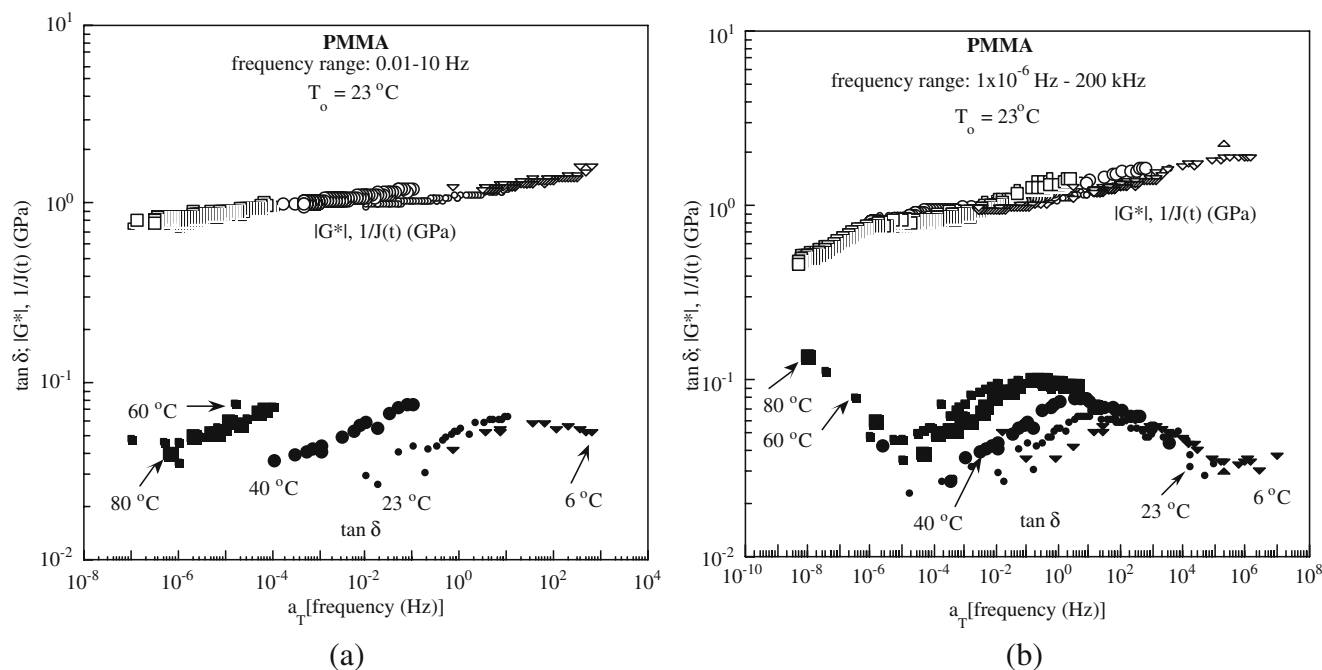


**Fig. 3** Master curve, reduced to 23°C, for PMMA comprised of a truncated data sets with frequency range from 0.01 to 10 Hz and **b** full data sets with frequency range from  $10^{-6}$  Hz to 200 kHz,

including RUS 23°C,  $\blacktriangle$ ,  $\triangle$ . *Solid symbols*,  $\tan \delta$ ; *open symbols*,  $|G^*|$ ,  $1/J(t)$ . 6°C, *inverted triangles*  $\blacktriangledown$ ,  $\triangledown$ ; 23°C, *small circles*  $\bullet$ ,  $\circ$ ; 40°C, *circles*  $\bigcirc$ ,  $\bullet$ ; 60°C, *small squares*  $\blacksquare$ ,  $\square$ ; 80°C, *large squares*  $\blacksquare$ ,  $\square$

data sets are used to create master curves, shown in Fig. 4.

The modulus curves over the full frequency range for both materials are shifted horizontally along the

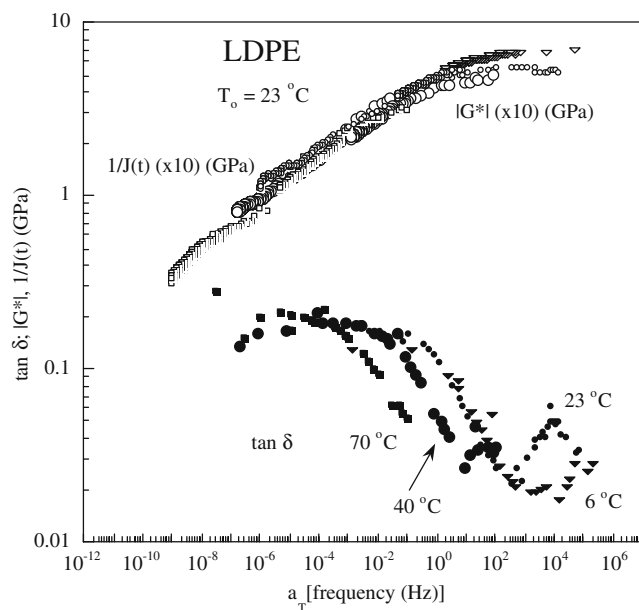


**Fig. 4** Master curve based on shifts to align the shear modulus curves for LDPE, reduced to 23°C comprised of the full range of viscoelastic results. 6°C, *inverted triangles*  $\blacktriangledown$ ,  $\triangledown$ ; 23°C, *small circles*  $\bullet$ ,  $\circ$ ; 40°C, *circles*  $\bigcirc$ ,  $\bullet$ ; 70°C, *squares*  $\blacksquare$ ,  $\square$

logarithmic time axis to successfully create a composite curve that resembles the shape of the room temperature data set. The shift factors necessary to align the modulus curves are plotted in Fig. 5. For PMMA in this glassy region, an Arrhenius approach was superior to a WLF curve based on parameters determined by others near  $T_g$ . The inferred activation energy is about 17 kcal/mol (71 kJ/mol). The LDPE modulus curve shifts also followed an Arrhenius relation, with an activation energy of about 18 kcal/mol (75 kJ/mol). The constants used in the WLF and Arrhenius equations to predict the dependence of shift factor on temperature empirically determined from prior experiments on these materials do not accurately predict the amount of shifting necessary to create the present composite curves. In the case of PMMA, this disparity could be due to the fact that the previous experiments (McLoughlin and Tobolsky 1952) were conducted at higher temperatures near the glass transition temperature of the material. Different internal friction mechanisms have been shown to be active at high temperatures and temperatures near room temperature. Predictions based on Arrhenius shifts from previous experiments (Sandiford and Willborn 1960) do not model the observed LDPE shift factors. However an Arrhenius form with a different activation energy fits the shift factor data quite well for the modulus vs. frequency curves. Crystalline polymers have



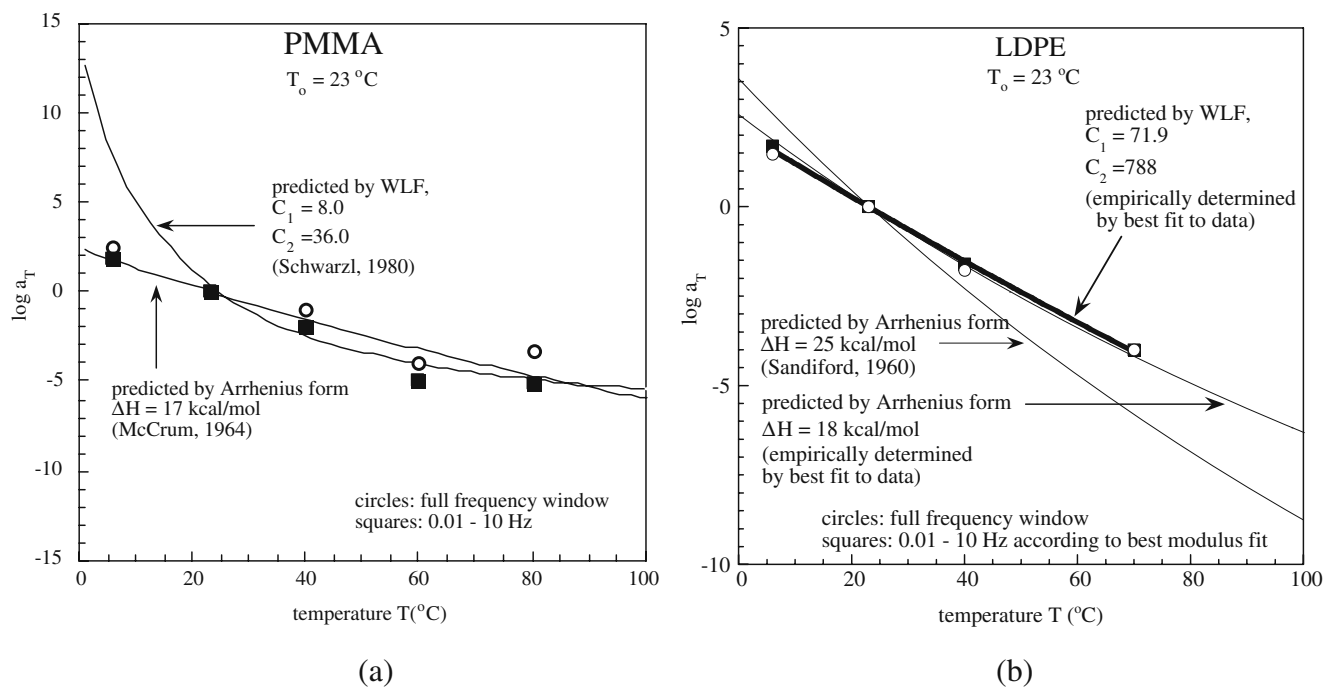


**Fig. 5** Time–temperature shift factor for PMMA **(a)** and LDPE **(b)** vs. temperature  $T$  and the predicted values of the shift factor dictated by the Arrhenius equation and the WLF equation. *Solid*

*squares* represent experimentally determined shift factors based on the abbreviated data set, *circles* represent experimentally determined shift factors based on the full frequency data set

multiple mechanisms overlapping in the same temperature region. The combined effects of these internal friction mechanisms is considered to be responsible for thermorheological complexity in crystalline polymers.

Although the master curve for modulus for both polymers shows reasonable alignment of the shifted curves, the loss tangent curves do not align with a simple horizontal shift along the time axis in the master curve plots. Deviation from time–temperature superposition is not surprising in LDPE since it is a partly crystalline polymer in which such deviations are well known. For example, Stadler et al. (2005) studied polyethylenes of various crystallinity over as much as 3.2 decades in frequency up to 10 Hz; they pointed out that papers describing the frequency dependence are scarce. For LDPE the  $\alpha'$  peak in  $\tan \delta$  increased in magnitude by about 8% from 20 to 50°C, and for HDPE the peak increased by about 25% from 65 to 135°C. The difference is attributed to the fact that for LDPE no other peaks are nearby but for HDPE the transition is just below the melting point and just above the  $\alpha$  transition. The  $\alpha'$  peak is attributed to the interface between crystal lamellae and amorphous interlamellar regions. Nitta and Tanaka (2001) concluded from temperature dependence of complex modulus that the position of both melting temperature and  $\alpha$  relaxation of polyethylene is inversely related to the lamellar

thickness. Wood-Adams and Costeux (2001) studied thermorheological complexity of polyethylene in the terminal zone, 130 to 190°C at 10 Hz. Modulus shift factors  $b_T$  were found to be much smaller in magnitude (about 1%) than those predicted by the Rouse model (about a 10% increase in modulus over 60°C). Shift factors  $a_T$  were developed based on the zero shear viscosity; these are not germane to the glassy regime studied here. Indeed, in the melt, the thermorheological complexity is the consequence of a different temperature dependence of different molecule types (Wood-Adams and Costeux 2001; Stadler et al. 2008). In the solid state, several phases are present (amorphous and crystalline), whose interaction and structure are temperature dependent (Mandelkern 1993; Hartwig 1994), giving rise to thermorheological complexity. Moreover, at the highest temperatures, there is the possibility of a physical aging or annealing of the crystalline structure, giving rise to thermorheological complexity.

Although it may be tempting to interpret the  $\alpha$  peak in damping of polyethylene as a result of glass transition, Stehling and Mandelkern (1970), based on rheological and thermal measurements, suggested that the glass transition is manifested in the  $\gamma$  transition near  $-130^\circ\text{C}$ . This is far below the temperatures reached in the present study. The subject has been a subject of some controversy;  $T_g$  may be the  $\beta$  transition,

masked in HDPE by effects of crystallinity. It is generally agreed that  $T_g$  of branched PE is distinctly below room temperature (that is certainly true, but whether  $T_g$  is  $-20$  or  $-130^\circ\text{C}$  is still uncertain). The problem lies in the complexity of the highly ordered PE superstructure, which makes a more detailed assessment very complicated.

The role of chain branching in polymer melts was explored by Carella et al. (1986) over a range of about 5.5 decades from 0.001 to 250 rad/s. The melts are thermorheologically complex; the activation energy is proportional to branch length. Such results may be pertinent to the complexity observed in the glassy regime, since the commercial polyethylene used in the present work is likely to contain a distribution of molecular environments. As for vertical shifts in the moduli (e.g., following the Rouse model), they apply to both the storage and loss moduli, so there is no effect on the loss tangent. Therefore, such shifts are inadequate to model the results observed here. Moreover, while there is a theoretical basis for such modulus shifts in the transition zone, the picture is less clear in the glassy zone, the subject of the present study. Indeed, Nakayasu et al. (1961) studied HDPE over some seven decades of frequency and found that vertical shifts spread the curves further apart and lessened the possibility of achieving superposition by horizontal shifts. Loss compliance  $J''$  curves superposed reasonably well from  $-29$  to  $15^\circ\text{C}$  but failed to superpose from  $15$  to  $70^\circ\text{C}$ .

In PMMA in the glassy region, Ferry (1970) expressed some caveats regarding time temperature shifts for modulus or compliance curves in the glassy region. Specifically, the slope of these curves is smaller in the glassy region than it is in the transition region, enhancing the relative role of small vertical shifts associated with temperature dependence of asymptotic moduli. The inference of a vertical shift factor from Rouse theory as is done in the transition and terminal zones does not apply in the glassy zone. Vertical shifts, if used, would apply to the modulus but not to  $\tan \delta$ . In any case, for a sufficiently broad frequency spectrum, one may expect a variety of secondary damping processes, each of which may have a different activation energy.

Heijboer (1977) pointed out that the  $\alpha$  and  $\beta$  peaks in glassy polymers have different activation energies. Therefore, if both peaks are present in a frequency window, thermorheological complexity will be manifest. Secondary peaks tend to follow an Arrhenius temperature dependence. For example, a  $\gamma$  peak in poly(cyclohexyl methacrylate) was observed using a variety of test devices as a function of temperature for

six discrete frequencies from  $10^{-4}$  Hz to 800 kHz. The position of the  $\tan \delta$  peak followed an Arrhenius dependence, but the peak height increased modestly with frequency, a fact not remarked upon. As for PMMA, the  $\beta$  peak is usually attributed to partial rotation of the COO group about the C–C bond which links the group to the main chain. The potential barrier is due to the adjacent methyl groups protruding from the chain. Substitution of other atoms or groups for methyl alters the temperature for the peak. Plazek (2007) recently surveyed experimental evidence of thermorheological complexity in polymers. He considered the role of the coupling model in explaining the breakdown of time–temperature superposition in the transition and terminal regions. In the present results in the glassy region, the PMMA  $\beta$ -damping peak increases in amplitude with increasing temperature and does not shift to a suitable alignment with the same shift factor as the modulus curves. At sufficiently high temperature, partial overlap of  $\alpha$  and  $\beta$  peaks could give rise to a failure of superposition. However, over the temperature range studied here, the tail of the  $\alpha$  peak rolls off too quickly even at  $80^\circ\text{C}$ , the highest temperature used, to significantly alter the  $\beta$  peak height. Therefore, it is suggested that such known deviations from time temperature superposition in PMMA do not suffice to explain the observed variation in the  $\beta$  peak height.

The inverse of the  $\beta$  peak maximum  $\tan \delta$  is plotted vs. temperature in Fig. 6. The linear dependence is suggestive of a Curie–Weiss temperature dependence

$$\tan \delta_{\max} = \frac{qT_0}{(T - T_0)} \quad (6)$$

with  $T_0$  as a critical temperature and  $q$  as a constant. Such temperature dependence of a physical property is indicative of energy associated with ordering of constituents in a material. Examples include the interaction of magnetic dipoles in paramagnetic materials and the interaction of solute atoms in polycrystalline metals (Zener 1948; Li and Nowick 1961). The latter interaction gives rise to  $\tan \delta$  peaks which change in magnitude with temperature according to Eq. 6 as well as shifting on the log frequency scale. This is the well-known Zener relaxation in which the magnitude of the peak  $\tan \delta$  is proportional to the square of the solute concentration (Nowick and Seraphin 1961). The Zener relaxation is considered to be a type of second-order transformation called an order–disorder transition (Benoit 2001). In  $\beta$  brass, for example, the body-centered cubic lattice can be regarded as two



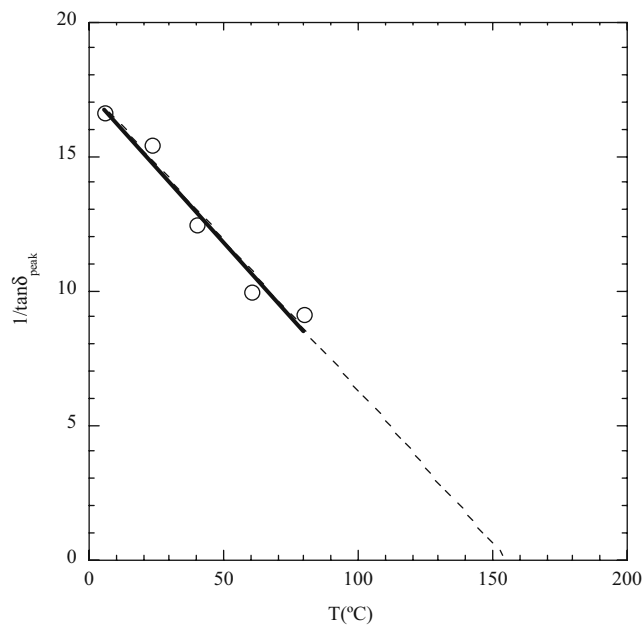


**Fig. 6** Inverse of  $\beta$  peak maximum  $\tan \delta$  vs. temperature  $T$  for PMMA. Circles: experiment, line, fit based on Curie–Weiss formula

interpenetrating simple cubic lattices. At low temperature, one of the lattices is preferentially occupied by one type of atom, e.g., copper. At a temperature above the critical temperature, the occupancy of lattice sites by specific atoms becomes disordered. Theory for this class of transformation predicts that the relaxation strength is highly sensitive to temperature. Therefore, to properly characterize such materials, it is necessary to measure the relaxation peak isothermally as a function of frequency rather than by temperature scans at one frequency. A similar mechanism in PMMA would entail an interaction between nearby side groups, the motion of which gives rise to the  $\beta$  peak. Indeed, Heijboer (1977) briefly considered intermolecular interactions in the context of polarity of the ester group but did not provide predictions of the consequences in the magnitude of the  $\beta$  peak.

The contrast between modulus curves and damping curves does not contradict the Kramers Kronig relations. These relations interrelate modulus and damping when both are known over a full range of frequency. They do not address the temperature variation of properties.

Broadband results do not always entail a breakdown of time temperature superposition. For example, a 80In15Pb5Ag solder alloy (Edwards et al. 2000) followed an Arrhenius relation from  $-6$  to  $50^\circ\text{C}$ , and superposition, corresponding to a shift of 1.9 decades,

was observed over nine decades of true frequency. The “high temperature” background damping (damping observed in polycrystalline materials at an absolute temperature  $T$  that is a significant fraction of the melting point) in crystalline metals appears to be governed by a combination of thermally activated dislocation mechanisms dominated by diffusion in the vicinity of grain and sub-grain boundaries. When diffusion dominates the damping, Arrhenius relations can apply over a wide range of frequency. Indeed, Arrhenius behavior has been observed over some 16 orders of magnitude in diffusion coefficient or more than a factor of four in absolute temperature (Weller 2006) based on the Snoek relaxation in crystalline metals.

To summarize, thermorheological complexity was observed in LDPE but that is not unexpected. The magnitudes of the damping peaks do not change much with temperature but the shapes change. Moreover, the damping peaks do not superpose when shift is done to align the modulus curves. If shift is applied to the loss tangent curves, they still do not align because their size and shape depends on temperature; moreover, the corresponding modulus curves then fail to align. This is attributed to the partly crystalline nature of this polymer in which deviations from time–temperature superposition are known to result from multiple relaxation mechanisms. In PMMA, the  $\beta$  peak increases in magnitude with temperature, a phenomenon which cannot be explained either by differences in activation energy for  $\alpha$  and  $\beta$  relaxations or by modulus shifts (e.g., based on Rouse models). Future studies to explore the notion of an order–disorder transition could vary the concentration of side groups responsible for the  $\beta$  relaxation. The rationale is that the magnitude of the damping peak via order–disorder transitions increases quadratically with concentration of species responsible for the damping.

## Conclusion

The present results characterize the dynamic behavior of LDPE and PMMA over a wider range of frequencies than has previously been possible with any single instrument, providing a critical test of time–temperature superposition. Shift factors used to align the shear modulus curves can follow an Arrhenius relation. The loss tangent curves do not shift by the same amount as the shear modulus curves. In the case of PMMA, the  $\beta$  damping peak increases in amplitude with temperature according to the Curie–Weiss formula. Such effects were not observed in previous creep or stress relaxation

studies on PMMA because these studies were restricted to low frequency or static loading conditions and were not capable of measuring  $\tan \delta$  over the full range of the  $\beta$  damping peak.

## References

- Benoit W (2001) Thermodynamics of phase transformations. In Schaller R, Fantozzi G, Gremaud G (eds) Mechanical spectroscopy  $Q^{-1}$ . Trans Tech, Switzerland, pp 341–360
- Brodt M, Cook LS, Lakes RS (1995) Apparatus for measuring viscoelastic properties over ten decades: refinements. *Rev Sci Inst* 66(11):5292–5297
- Carella JM, Gotro JT, Graessley WW (1986) Thermorheological effects of long-chain branching in entangled polymer melts. *Macromolecules* 19:659–667
- Cavaille JY, Corinne J, Perez J, Monnerie L, Johari GP (1987) Time–temperature superposition and dynamic behavior of atactic polystyrene. *J Polym Sci: Part B Polym Phys* 25: 1235–1251
- Edwards LK, Nixon WA, Lakes RS (2000) Viscoelastic behavior of 80In15Pb5Ag and 50Sn50Pb alloys: experiment and modeling. *J Appl Phys* 87(3):1135–1140
- Ferry JD (1950) Mechanical properties of substances of high molecular weight. VI dispersion in concentrated polymer solutions and its dependence of temperature and concentration. *J Am Chem Soc* 72:3746–3752
- Ferry JD (1970) Viscoelastic properties of polymers. Wiley, New York
- Flocke HA (1962) Ein Beitrag zum mechanischen Relaxationsverhalten von Polyäthylen, Polypropylen, Gemischen aus diesen und Mischpolymerisaten aus Propylen und äthylen. *Kolloid-Z* 180:118–126
- Hartwig G (1994) Polymer properties at room and cryogenic temperatures. Plenum, New York
- Heijboer J (1977) Secondary loss peaks in glassy amorphous polymers. *Int J Polym Mat* 6:11–37
- Koppelman VJ (1958) Über die Bestimmung des dynamischen Elastizitätsmoduls und des dynamischen Schubmoduls im Frequenzbereich von  $10^{-5}$  bis  $10^{-1}$  Hz. *Rheol Acta* 1:20–28
- Lakes RS (1999) Viscoelastic solids. CRC Press, Boca Raton, FL
- Lee T, Lakes RS, Lai A (2000) Resonant ultrasound spectroscopy for measurement of mechanical damping: comparison with broadband viscoelastic spectrosc. *Rev Sci Instrum* 71: 2855–2861
- Li CY, Nowick AS (1961) Magnitude of the Zener effect—II. Temperature dependence of the relaxation strength in  $\alpha$  Ag-Zn. *Acta Metall* 9:49–58
- Mandelkern L (1993) The crystalline state, 2nd edn. Chap. 4. ACS, Washington DC
- Marvin RS (1953) The dynamic mechanical properties of polyisobutylene. In: Proceedings of the second international congress of rheology, London, pp 156–163
- McCrum NG, Buckley CP, Bucknall CB (1997) Principles of polymer engineering. Oxford University Press, Oxford
- McLoughlin JR, Tobolsky AV (1952) The viscoelastic behavior of polymethyl methacrylate. *J Colloid Sci* 7:555–568
- Nakayasu H, Markovitz H, Plazek DJ (1961) The frequency and temperature dependence of the dynamic mechanical properties of a high density polyethylene. *J Rheol* 5:261–283
- Nitta K-H, Tanaka A (2001) Dynamic mechanical properties of metallocene catalyzed linear polyethylenes. *Polymer* 42:1219–1226
- Nowick AS, Seraphim DP (1961) Magnitude of the Zener relaxation effect I. Survey of alloy systems. *Acta Metall* 9:40–48
- Plazek DJ (1980) The temperature dependence of the viscoelastic behavior of poly (vinyl acetate). *Polym J* 12:43–45
- Plazek DJ, Chay I, Ngai KL, Roland CM (1995) Viscoelastic properties of polymers. 4. Thermorheological complexity of the softening dispersion in polyisobutylene. *Macromolecules* 28:6432–6436
- Plazek DJ (2007) Anomalous viscoelastic properties of polymers: experiments and explanations. *J Non-Crystalline Solids* 353:3783–3787
- Sandiford DJH, Willborn AH (1960) Polythene. Iliffe, London
- Stadler FJ, Kaschta J, Münstedt H (2005) Dynamic-mechanical behavior of polyethylenes and ethene-/ a-olefin-copolymers. Part I.  $\alpha$ -Relaxation. *Polymer* 46:10311–10320
- Stadler FJ, Kaschta J, Münstedt H (2008) Thermorheological behavior of long-chain branched metallocene catalyzed polyethylenes. *Macromolecules* 41(4):1328–1333
- Stehling FC, Mandelkern L (1970) The glass temperature of linear polyethylene. *Macromolecules* 3:42–252
- Tobolsky AV, Andrews RD (1945) Systems manifesting superposed elastic and viscous behavior. *J Chem Phys* 13:3–27
- Weller M (2006) The Snoek relaxation in bcc metals—from steel wire to meteorites. *Mat Sci Eng A* 442:21–30
- Wood-Adams P, Costeux S (2001) Thermorheological behavior of polyethylene: effects of microstructure and long chain branching. *Macromolecules* 34:6281–6290
- Zener C (1948) Elasticity and anelasticity of metals. University of Chicago Press, Chicago